doi.org/10.36721/PJPS.2025.38.3.REG.13065.1

Anti-cancer effects of *Trifolium pratense* L. on hepatocellular carcinoma via the HOTAIR/miR-124/Notch1 pathway: A biochemical and histopathological study in rats

Chao-Du[1#], Rubing-Deng[2#], Ji-Li[3] and Yanfei-Wang[3]*

[1]Department of Hepatobiliary Surgery, The Third Affiliated Hospital of Zunyi Medical University. The First People's Hospital of Zunyi, Zunyi City, Guizhou Province, China.

[2]Department of General Surgery, The First People's Hospital of Longquanyi District, Chengdu (West China Longquan Hospital Sichuan University), Chengdu City, Sichuan Province, China.

[3]Department of Hepatobiliary Surgery, People's Hospital of HeChuan Chong Qing, Chongqing City, China.

Abstract: This research explored the protective effects of *Trifolium pratense* L. flower extract (TPFE) on hepatocytes against hepatocellular carcinoma (HCC) induced by N-diethylnitrosamine (DEN). The study focused on biochemical, molecular and antioxidant pathways, particularly the HOTAIR/miR-124/Notch1 axis. Fifty Wistar rats were divided into five groups: A normal control, an HCC-induced group (DEN 100mg/kg), two HCC groups treated with TPFE (200 mg/kg and 400mg/kg) and a normal group treated with TPFE (400mg/kg). At the study's end, liver function markers, inflammatory cytokines and oxidative stress parameters were measured. The expression of HOTAIR, miR-124, Notch1, and Jagged1 genes and proteins in liver tissue was assessed, along with immunohistochemical analysis for P53-positive cells. DEN administration led to significant alterations in body and liver weight, serum liver enzymes, antioxidant levels, inflammatory markers and gene/protein expression related to the HOTAIR/miR-124/Notch1 axis. Statistical analysis was performed using ANOVA, Newman-Keuls test and SPSS, with significance at $p<0.05$; data visualized in GraphPad. TPFE treatment mitigated these changes in a dose-dependent manner, particularly at 400mg/kg, improving weight, liver health, antioxidant capacity and inflammatory responses. Histopathological and immunohistochemical analyses showed structural liver improvements with TPFE. The study concludes that TPFE has potential anti-cancer effects against DEN-induced HCC.

Keywords: Trifolium pratense L., N-diethylnitrosamine, HOTAIR, liver, hepatocellular carcinoma.

Submitted on 03-07-2024 – Revised on 02-10-2024 – Accepted on 17-10-2024

INTRODUCTION

Hepatocellular carcinoma (HCC) is the most prevalent liver cancer, with 500,000 to 1,000,000 new cases annually, causing around 600,000 deaths. Asia has the highest incidence rates (20-40 per 100,000 annually), while Europe has lower rates (3-15 per 100,000 annually), according to WHO reports (Konyn *et al.,* 2021). Genetic mutations, including deletions of tumor suppressors (PTEN, p53, CDKN2B) and amplifications of oncogenes (MET, MYC, FGF19), along with alterations in pathways like Notch, PI3K/AKT/mTOR, p53/p21, HOTAIR/Notch1, Wnt/β-catenin and JAK/STAT, significantly influence tumor development by affecting metabolism, cell cycle, repair mechanisms, angiogenesis, and immune responses (Sumislawski *et al*., 2022). Major HCC risk factors are viral hepatitis (B and C), toxin exposure (aflatoxins, alcohol, chemotherapy drugs), metabolic conditions (fatty liver disease, diabetes, hereditary hemochromatosis) and immune disorders. Pro-inflammatory cytokines [IL-6, IL-1β, IL-10, tumor necrosis factor- α (TNF-α)], reactive oxygen species (ROS) and reactive nitrogen species (RNS) create a tumor-promoting microenvironment (Fathi *et al*., 2021).

Nitrosamines, including N-diethylnitrosamine (DEN), are organic carcinogens found in tobacco, vehicle exhaust, cosmetics, canned foods and cooked or fried foods. These compounds cause DNA damage in normal cells, leading to tumors in organs such as the liver, colon, nose, lung, and pancreas (Balaraman *et al*., 2021). DEN, specifically, is used in research to induce liver tumors in animal models. Administered through injection or gavage, DEN causes liver toxicity, chronic inflammation, fibrosis and at higher doses, liver tumors. Its carcinogenicity is linked to elevated G1/S-phase regulatory proteins and biotransformation into alkylating metabolites that damage DNA. This process generates ROS and RNS, disrupting free radical balance and damaging cellular components like proteins and lipids (Chen *et al*., 2021).

HOX transcript antisense RNA (HOTAIR), a long non-coding RNA associated with various cancers, including liver cancer, regulates gene expression and epigenetics. In liver cancer, miR-124, a microRNA, controls proliferation, invasion and metastasis, with dysregulation contributing to disease progression (Giovannini *et al*.,

**Corresponding authors:* e-mails: wangyanfei2023@sina.com

2021). Notch1, a transmembrane receptor crucial for cell signaling related to proliferation, differentiation and apoptosis, is implicated in liver cancer through abnormal pathway activation. Jagged1, a Notch receptor ligand, activates the Notch pathway, promoting tumor growth and metastasis, leading to poor prognosis. Current research explores these molecules' roles and interactions, offering potential therapeutic targets (Xiao *et al*., 2022).

Trifolium pratense L. flower extract (TPFE), from the fabaceae family, is globally distributed, particularly in Eastern Europe, Northern Africa, and Asia. TPFE contains 25-35% starch, 5% mucilage, 10% saccharose, 11% pectins and polyphenols like catechin, formononetin, biochanin A, genistein and daidzein. It also includes phytosterols, coumarins, asparagine, tannins and scopoletin (Jing *et al*., 2021). Traditionally, TPFE has been used in soups, teas and as a food additive to treat dry coughs, flatulence, diabetes, hyperlipidemia, diarrhea, fever, and boost immunity. Modern medicine uses TPFE for cardiovascular diseases, respiratory infections, urolithiasis prevention and immune and estrogenic modulation (Akbaribazm *et al*., 2020a). TPFE acts as an antioxidant and apoptosis inducer, enhancing glutathione-S-transferase (GST) gene expression and inhibiting proliferation in prostate cancer cells. Isoflavones in TPFE suppress tumor cell growth in vitro and in vivo (Antonescu *et al*., 2021). Studies have demonstrated that TPFE regulates biochemical indicators of liver function, including alkaline phosphatase (ALP), albumin (ALB), alanine aminotransferase (ALT), C-reactive protein (CRP), total protein (TP), aspartate aminotransferase (AST), and bilirubin (BIL), through its antioxidant and anti-inflammatory properties in ovariectomized rats (Quah *et al*., 2022). Studies have shown that the isoflavonoid compounds formononetin, biochanin A, genistein and daidzein present in TPFE regulate hepatocyte function and related biochemical indices through various pathways, including the suppression of oxidative stress, the Nrf2 pathway and the PI3K/Akt/mTOR pathway (Zughaibi *et al*., 2021). Additionally, these compounds can inhibit the release of inflammatory cytokines through anti-inflammatory pathways involving cyclooxygenase-2 (COX-2)/IL-6, ultimately regulating the biochemical indices of hepatocytes (Wu *et al*., 2021).

Our investigation explores TPFE's anti-tumor effects against DEN-induced HCC in Wistar rats, focusing on antioxidative, anti-inflammatory, mitochondrial apoptosis, and HOTAIR/miR-124/Notch1 signaling pathways.

MATERIALS AND METHODS

Preparation of TPFE

The freshly harvested flowers of Trifolium pratense L. in Chongqing city research farm, weighing 4000 grams, were dried at 35°C in a dark environment, with confirmation by a botanist. Subsequently, the dried leaves underwent grinding into a powder using a soil grinder. The powdered leaves were then combined with 70% ethanol (30:70 distilled water (DW) / ethanol). After 72 hours of incubation at 35°C, the mixture was filtered through a paper filter and subsequently compressed using a rotary evaporator. The resulting extract, totaling 350 grams, was stored at 4°C (Akbaribazm *et al*., 2020b).

Experimental design

Fifty male Wistar rats, weighing on average 220±20 grams, were randomly allocated into 5 groups (n=10/group). Prior to commencement of the study, a 72-hour adaptation period was provided to allow the rats to acclimate to the study conditions, including temperature, food, and water availability. Throughout the study duration, all rats were housed in propylene cages maintained at a temperature of 22±3°C, with a relative humidity of 45±5%, and subjected to a 12-hour light/12-hour dark cycle. Standard rat pellets and tap water were provided ad libitum to all groups.

In the study, the normal group received an intraperitoneal injection of 500 µl PBS, while the HCC group received an intraperitoneal injection of 100mg/kg DEN dissolved in 500µl PBS. The co-treatment groups (HCC+200 and HCC+400 TPFE) received oral administration of DEN along with 200 and 400mg/kg of TPFE, respectively. Additionally, the normal+400 TPFE group received 400 mg/kg of TPFE orally. The effective dose for the non-toxic treatment was determined using the LD_{50} method, alongside preliminary studies and existing research on DEN and TPFE. Administration of DEN and TPFE was conducted daily at fixed times, 9 am and 3 pm, respectively (Khazaei *et al*., 2022; Zhang *et al*., 2021a).

LD_{50} for TPFE

The determination of TPFE's LD50 was conducted using Lork's two-step method. Initially, nine rats were divided into three groups and administered doses of 50, 500, and 5000mg/kg of TPFE, respectively. These rats were closely monitored for any signs of mortality or toxicity over a 24-hour period. Subsequently, another set of three rats per group received doses of 10, 100 and 1000mg/kg of TPFE, respectively, and were similarly observed within the same timeframe. The LD_{50} was calculated using Lork's formula, which considers both the highest safe dose (SD) and the lowest dose resulting in mortality (toxic dose, TD) observed during the monitoring period. $LD_{50} = (DTD \times DSD)\ 1/2$ (Khordad *et al*., 2024).

Serum levels of alkaline phosphatase (ALP), albumin (ALB), alanine aminotransferase (ALT), C-reactive protein (CRP), total protein (TP), aspartate aminotransferase (AST) and bilirubin (BIL)

After completing the study, euthanasia of the rats was performed using a combination of pre-anesthesia and

anesthesia. This involved intraperitoneal injection of 80 mg/kg of 2% xylazine and 60 mg/kg of 10% ketamine. Subsequently, blood samples were collected from the heart, and serum was separated by centrifugation. The levels of AST, BIL, CRP, ALT, ALP, TP and ALB in the serum were quantified using ELISA kits obtained from a commercial supplier, following the manufacturer's guidelines (Al-Attar *et al*., 2022).

Serum glutathione peroxidase (GPx), catalase (CAT), and superoxide dismutase (SOD) activity

We utilized a sandwich-based ELISA kit specifically designed for rodents, sourced from Cusabio in China, to assess the serum levels of glutathione peroxidase (GPx; Cat. No.: CSB-E12146r), catalase (CAT; Cat. No.: CSB-E13439r) and super oxide dismutase (SOD; Cat. No.: CSB-EL022397RA), following the manufacturer's instructions (Wang *et al*., 2022a).

Serum levels of nitric oxide (NO)

The Griess colorimetric method was utilized to assess serum nitric oxide (NO) levels, an important marker of lipid peroxidation and oxidative stress. Briefly, 500µl of serum samples were combined with 6 mg of zinc oxide, thoroughly mixed and centrifuged at 10,000 g for 15 minutes. The resulting supernatant was then mixed with 500µl of Griess solution. After incubating for 60 minutes at 37°C, the absorbance of the mixture was measured using an ELISA reader (Stat Fax ELISA reader, model number: 303 microwell readers, manufactured by Awareness Technology, United States) at wavelengths of 540 nm and 630 nm (Al-Attar, 2022).

Liver tissue thiol levels, total antioxidant capacity (FRAP levels) and lipid peroxidation levels (TBARS levels)

One method used to assess total antioxidant capacity is the ferric reducing antioxidant power (FRAP) analysis. In summary, 100 mg of liver tissue was homogenized at 4°C and then mixed with 200µl of cold PBS. From this mixture, 100µl was combined with 10µl of FRAP solution. After incubating the extract at 25°C for 15 minutes and centrifuging at 12,000g for 10 minutes, the absorbance of the resulting supernatant was measured at 593 nm using an ELISA reader (Stat Fax ELISA reader, model number: 303 microwell readers, from Awareness Technology, United States).

Another approach to quantify levels of lipid peroxidation involves assessing liver tissue thiobarbituric acid reactive substances (TBARS). Initially, 100µl of homogenized liver tissue mixture was combined with 100µl of TBARS solution, followed by incubation at 37°C for 30 minutes and centrifugation at 12,000 g for 5 minutes. The absorbance of the resulting supernatant was then measured at 593 nm using an ELISA reader.

For determining liver tissue thiol levels, which serve as a critical index of tissue antioxidants, 100µl of homogenized liver tissue mixture was mixed with 20µl of 5,5-dithio-bis-(2-nitrobenzoic acid) (DTNB), followed by incubation at 37°C for 15 minutes and subsequent centrifugation at 12,000 g for 5 minutes. The absorbance of the supernatant was measured at 412 nm using an ELISA reader (Akbaribazm *et al*., 2020b).

IL-10, IL-1β, TNF-α and IL-6 serum levels

To assess the anti-inflammatory properties of TPFE extract, we measured the concentrations of pro-inflammatory cytokines [TNF-α (Cat. No.: NBP2-DY410), IL-6 (Cat. No.: M6000B), and IL-1β (Cat. No.: RLB00)], as well as the anti-inflammatory cytokine IL-10 (Cat. No.: R1000), using sandwich-style ELISA kits designed for rodents obtained from Novus Biologicals (United States). These analyses were conducted following the manufacturer's protocols (Al-Attar, 2022).

Jagged1, miR-124, HOTAIR and Notch1 genes expression

Liver tissue total RNA extraction was carried out using EX6101-RNX Plus Solution (Cat. No.: EX6101-RNX; SinaClon BioScience, China). Initially, cell lysis was induced by adding RNX Plus buffer, followed by the addition of 200µl of chloroform. The subsequent centrifugation at 13,000 g for 15 minutes at 4°C facilitated phase separation, resulting in a supernatant. This supernatant was then combined with cold isopropanol (200µl) and incubated on ice for 15 minutes, followed by another round of centrifugation at 13,000 g for 15 minutes. Afterward, 1 ml of 50% ethanol was added to the samples, which were centrifuged for 15 minutes at 13,000 g at 4°C. The resulting pellet was finally re-suspended in 50µl of distilled water and stored at -80°C.

For cDNA synthesis, the Revert AidTM First Strand cDNA Synthesis Kit (Cat. No.: K1621; Fermentas, USA) was employed, following the manufacturer's instructions. The sequences of HOTAIR, miR-124, Notch1, and Jagged1 genes were designed using Gene Runner software (Hastings Software, Hudson, United States). Following the design phase, the genes underwent a BLAST search in the NCBI database (https://www.ncbi.nlm.nih.gov/tools/primer-blast/) for validation. The GAPDH gene was selected as the internal reference, and the primer sequences were as follows: GAPDH (forward: TGAAGGTCGGAGTCAACGG, reverse: AGAGTTAAAAGCAGCCCTGGTG), HOTAIR (forward: GGTAGAAAAAGCAACCACGAAGC, reverse: ACATAAACCTCTGTCTGTGAGTGCC), Jagged1 (forward: CGCCCTCTGAAAAACAGAAC, reverse: ACCCAAGCCACTGTTAAGACA), Notch1 (forward: CTGGACCCCATGGACATC, reverse: ACTGTACACACTGCCGGTTG) and miR-124 (forward:

GGAACCTTCTGAGTGCCTTAC, reverse: CCGTAAGTGGCGCACGGAAT). Gene amplification was conducted using forward and reverse primers under 42 temperature cycles on a Corbett Rotor thermocycler, with each cycle including 5 minutes at 70°C as the annealing temperature. The relative expression levels of the genes were determined using the threshold cycle (Ct) of each gene, ΔΔCt, and the fold change formula: ΔΔCt = [(Ct sample - Ct GAPDH gene) - (Ct sample - Ct control)]. The fold formula change = $2^{-\Delta\Delta CT}$ (Akbaribazm *et al*., 2020b).

Expression Jagged1, miR-124, HOTAIR and Notch1 proteins in liver with western blotting

To evaluate the protein expression levels of HOTAIR, miR-124, Notch1 and Jagged1, Western blot analysis was conducted. Initially, a homogenized liver tissue sample weighing 100 mg was prepared, mixed with 50µl of phosphate buffered saline (PBS) and 100µl of radio-immunoprecipitation assay buffer. After centrifugation, 20 µl of loading buffer was added to the polyvinylidene fluoride (PVDF) membrane, which was subsequently probed with primary antibodies obtained from Abcam, UK: HOTAIR (Cat. No. ab062614; 1:400), Notch1 (Cat. No. ab114178; 1:500), Jagged1 (Cat. No. ab152171; 1:500), and miR-124 (Cat. No. ab0616241; 1:500). The membrane was then subjected to separation on a 10% sodium dodecyl sulfate (SDS) polyacrylamide gel using appropriate techniques.

After incubating overnight at 4°C, the membrane was further incubated with a horseradish peroxidase (HRP) - conjugated secondary antibody for 40 minutes at 37°C. Finally, the signals from the protein bands were captured and analyzed using Bio-Rad software, utilizing an enhanced chemiluminescence reagent from e-BLOT company, China. Additional analysis was performed using Image J software (Zhang *et al*., 2021b).

Immunohistochemistry (IHC) assay

To detect p53-positive cells in liver tissues as an indicator of apoptotic differentiation within tumor cells, the following procedure was employed: Liver tissues were washed with PBS and processed using standard tissue processing techniques, resulting in the preparation of paraffin blocks. Sections measuring 5 µm were mounted on slides and underwent overnight incubation at 95°C with primary p53 antibodies (dilution 1:500; Cat. No.: GAF1355, R&D Systems, Inc., US). Subsequently, the slides were incubated for 1 hour at 25°C. Tween-20 was used as the washing buffer and residual antibodies were blocked with 5% bovine serum albumin.

The slides were then treated with 3% hydrogen peroxide (H_2O_2) for 20 minutes at 25°C, followed by staining with 3,3'-diaminobenzidine (DAB). Hematoxylin was utilized for counterstaining on all slides. An optical microscope (Model No. BX61TRF; Olympus, Japan) connected to Image J software facilitated examination of the slides at a magnification of 400X in ten randomly selected fields (Akbaribazm *et al*., 2020b).

Liver histopathology

The liver tissues were initially fixed in 10% formalin for 72 hours, followed by a gentle rinse with PBS. Subsequently, the samples underwent dehydration in progressively increasing concentrations of ethanol, clarification in xylene, and embedding in paraffin wax. Sections of 5µm thickness were then obtained from the paraffin blocks using a microtome (Model No. SM2010RV1.2 microtomes, LEICA, Germany) and dried in an incubator at 37˚C. Slides were prepared for hematoxylin and eosin (H&E) staining. Histological examination of the slides was performed using a light microscope at ×400 magnification. Images were captured using a calibrated light microscopic system (Model No. BX61TRF; Olympus, Japan) and analyzed using ImageJ software (Akbaribazm *et al*., 2020b).

Ethical approval

The research protocol involving animal experimentation received approval from The research protocol involving animal experimentation received approval from the third affiliated hospital of Zunyi medical university, the first people's hospital of Zunyi [approval No. (2024)-1-45)].

STATISTICAL ANALYSIS

To compare the quantitative results across the groups under study, statistical analysis was performed using one-way analysis of variance (ANOVA) followed by the Newman-Keuls post hoc test. Statistical significance was defined at $p<0.05$. The normality and homogeneity of the data were assessed using the Kolmogorov-Smirnov test, where a p-value greater than 0.05 indicated normal distribution and homogeneity. All data are presented as means ± standard deviation (SD). Data analysis was conducted using SPSS software (Version 16; IBM Inc., US), and GraphPad Prism software (Version 9; GraphPad Inc., US) was used for graphical representation of the results.

RESULTS

LD_{50} of TPFE

After a 24-hour observation period of the groups treated with TPFE, the results indicated that a dose of 1000 mg/kg was safe (DS), while a dose of 5000 mg/kg was found to be toxic (TD). Using Lork's formula, the LD_{50} of TPFE was calculated to be 2236.1 mg/kg. This suggests that in animal studies, doses below the LD_{50} of TPFE are suitable for use.

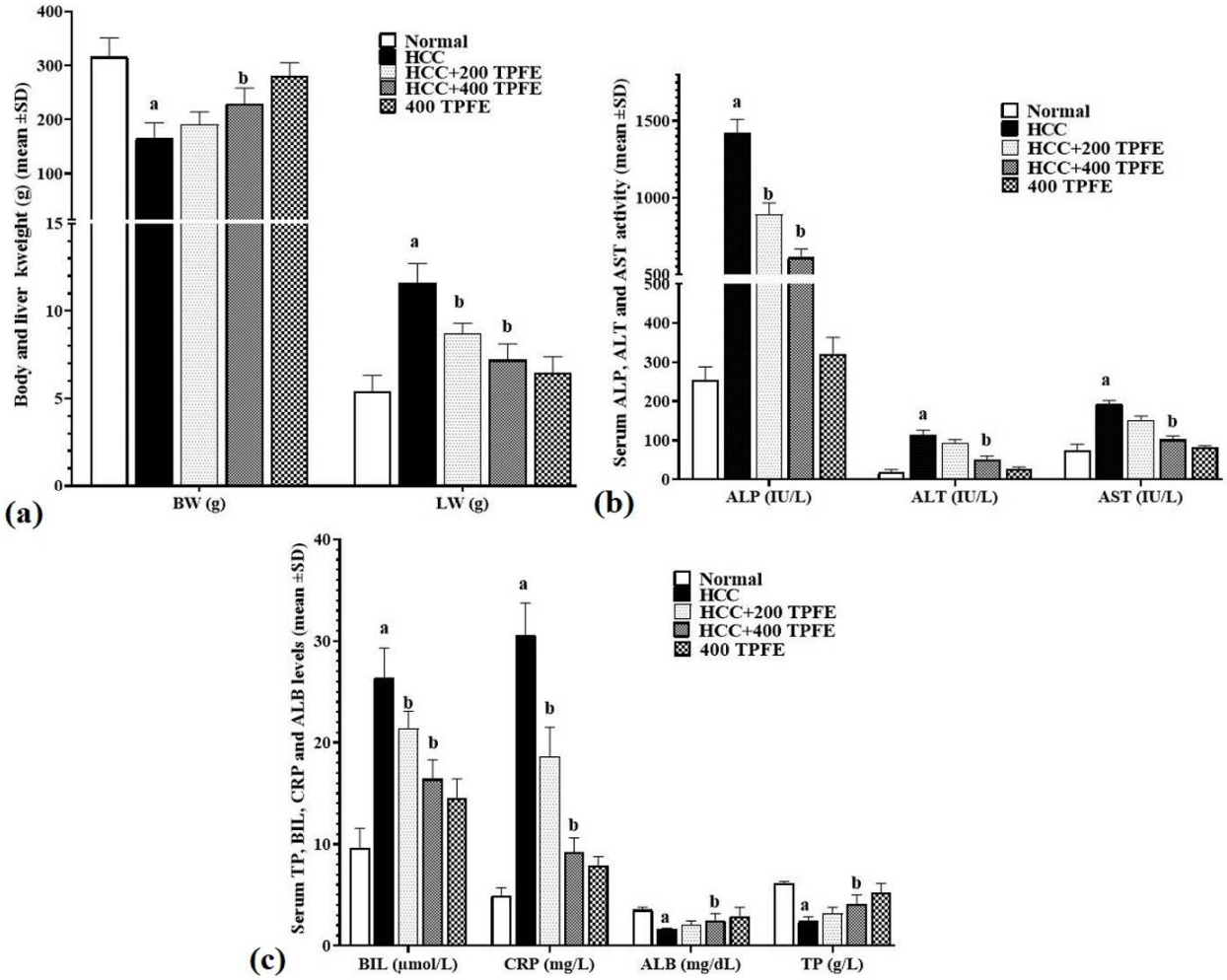

Fig. 1: (a) Rats body (BW) and liver (LW) (g) weight, (b) Serum activity of alanine aminotransferase (ALT), aspartate aminotransferase (AST) and alkaline phosphatase (ALP) enzymes (IU/L) and (c) serum levels of albumin (ALB) (mg/dL), total protein (TP) (g/L) and bilirubin (BIL) (μmol/L), C reactive protein (CRP) (mg/L) in experimental groups (means ± SD; n=10/group). a($p<0.05$) HCC vs. normal groups; b($p<0.05$) HCC+200 and 400 TPFE treated vs. HCC groups.

Body (BW) and liver (LW) weight

After examining the results related to BW and LW, it was observed that in the HCC group, DEN induced a significant decrease in BW ($p<0.05$) and a marked increase in LW ($p<0.05$) compared to the normal group. In contrast, administering TPFE at doses of 200 and 400 mg/kg in the HCC+200 and HCC+400mg/kg TPFE groups produced a dose-dependent effect. This resulted in a significant increase in body weight ($p<0.05$) and a notable decrease in liver weight compared to the HCC group (fig. 1a).

Biochemical analysis

Effects of TPFE and DEN on serum liver biochemical parameters

After assessing the activities of serum liver enzymes (ALT, AST and ALP), it was found that DEN significantly ($p<0.05$) elevated the activity levels of all three enzymes compared to the normal group. In the treatment groups (HCC+200 and 400mg/kg TPFE), there was a significant reduction ($p<0.05$) in the activity levels of these enzymes compared to the HCC group (fig. 1b). The analysis of serum BIL and CRP data showed a significant increase ($p<0.05$) in both indicators in the HCC group compared to the control group. Notably, TPFE demonstrated a dose-dependent effect in decreasing ($p<0.05$) the levels of these serum indicators compared to the HCC group. Evaluation of serum ALB and TP levels across the groups revealed that DEN significantly ($p<0.05$) reduced the levels of both markers compared to the control group. Conversely, the HCC+400mg/kg TPFE treatment group showed a significant increase ($p<0.05$) in the levels of these markers compared to the HCC group (fig. 1c).

Serum levels of TNF-α, IL-10, IL-6 and IL-1β

DEN triggered inflammatory responses, leading to an increase in the concentration of pro-inflammatory cytokines and a reduction in the activity of systemic anti-

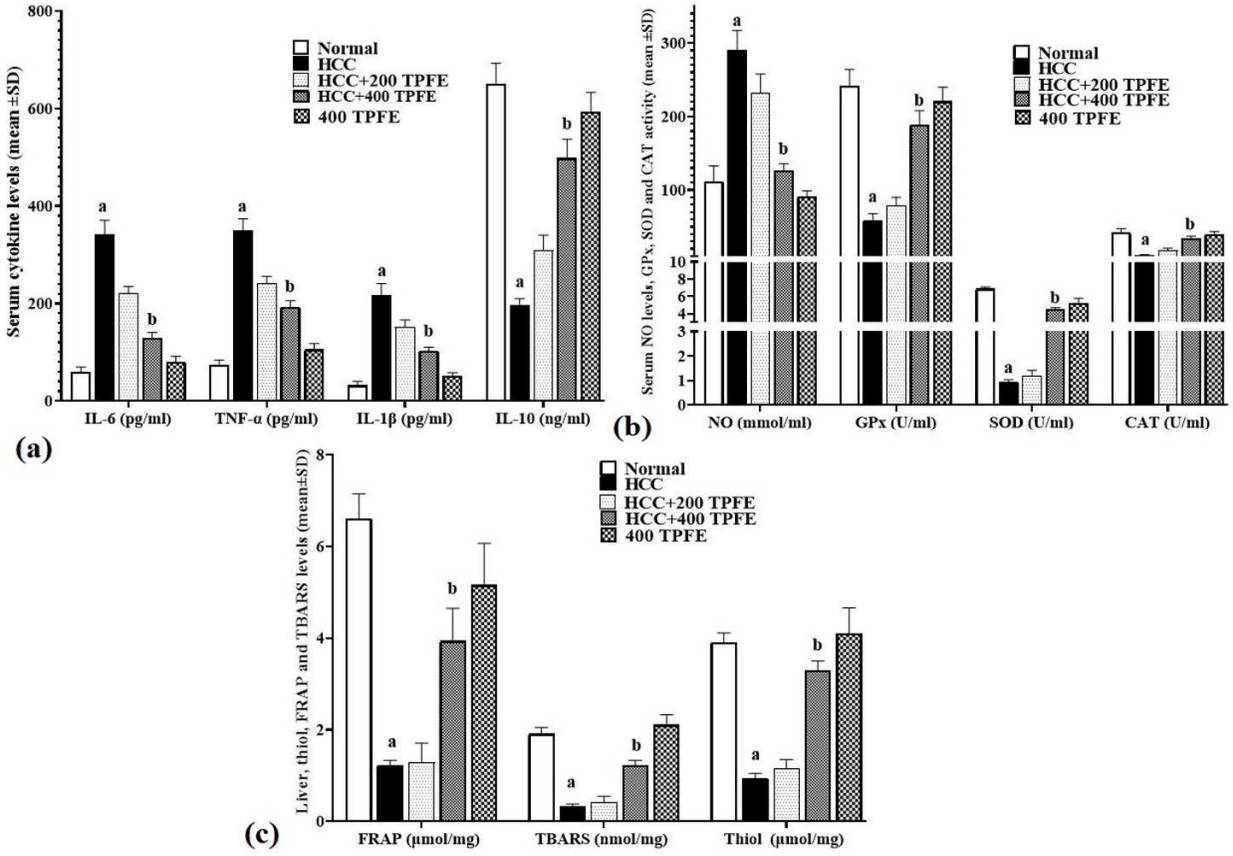

Fig. 2: (a) Serum levels of IL-1β, TNF-α, IL-6 (pg/ml) and IL-10 (ng/ml) (b) Serum levels of NO (mmol/ml), alongside the mean serum activity of SOD, CAT and GPx (U/ml) and (c) Liver tissue levels of TBARS (nmol/mg) and FRAP (µmol/mg) (means ± SD; n=10/group) in experimental groups. [a]($p<0.05$) HCC vs. normal groups; [b] ($p<0.05$) HCC+200 and 400 TPFE treated vs. HCC groups.

inflammatory cytokines. This resulted in a significant elevation ($p<0.05$) in the serum levels of the pro-inflammatory cytokines TNF-α, IL-1β and IL-6 compared to the normal group, while the level of IL-10 significantly decreased. However, the study findings highlighted the potent anti-inflammatory properties of TPFE. It progressively increased the serum levels of IL-10 and decreased the levels of TNF-α, IL-1β and IL-6 compared to the HCC group. These changes were statistically significant ($p<0.05$) at a dosage of 400 mg/kg (within the HCC+400 TPFE group) compared to the HCC group (fig. 2a).

Serum GPx, CAT and SOD activity alongside serum NO levels

DEN, by inducing free radical production, significantly increased serum NO levels compared to the normal group. Conversely, TPFE showed a dose-dependent decrease in NO levels compared to the DEN group, with a statistically significant reduction ($p<0.05$) at a dosage of 400 mg/kg (within the HCC+400 TPFE group). Additionally, DEN significantly reduced the serum activity of all three antioxidant enzymes compared to the control group. In contrast, TPFE increased the serum levels of all three enzymes in a dose-dependent manner compared to the control group, with a statistically significant increase ($p< 0.05$) observed at a dosage of 400mg/kg (within the HCC+400 TPFE group) compared to the HCC group (fig. 2b).

Thiol, FRAP and TBARS levels in liver

The levels of Thiol, FRAP and TBARS served as crucial markers for assessing the overall antioxidant capacity and lipid peroxidation. The study findings indicated that DEN significantly ($p<0.05$) decreased the levels of all three parameters in the tissues compared to the control group. In contrast, TPFE, recognized for its strong antioxidant properties, demonstrated a dosage-dependent elevation in these parameters compared to the DEN-exposed group. This increase was statistically significant ($p<0.05$) at the 400mg/kg dose (within the HCC+400 TPFE group) in comparison to the HCC group (fig. 2c).

Molecular assay

Expression of liver HOTAIR, miR-124, Notch1 and Jagged1 genes

The examination of gene expression linked to proliferation, differentiation and apoptosis pathways

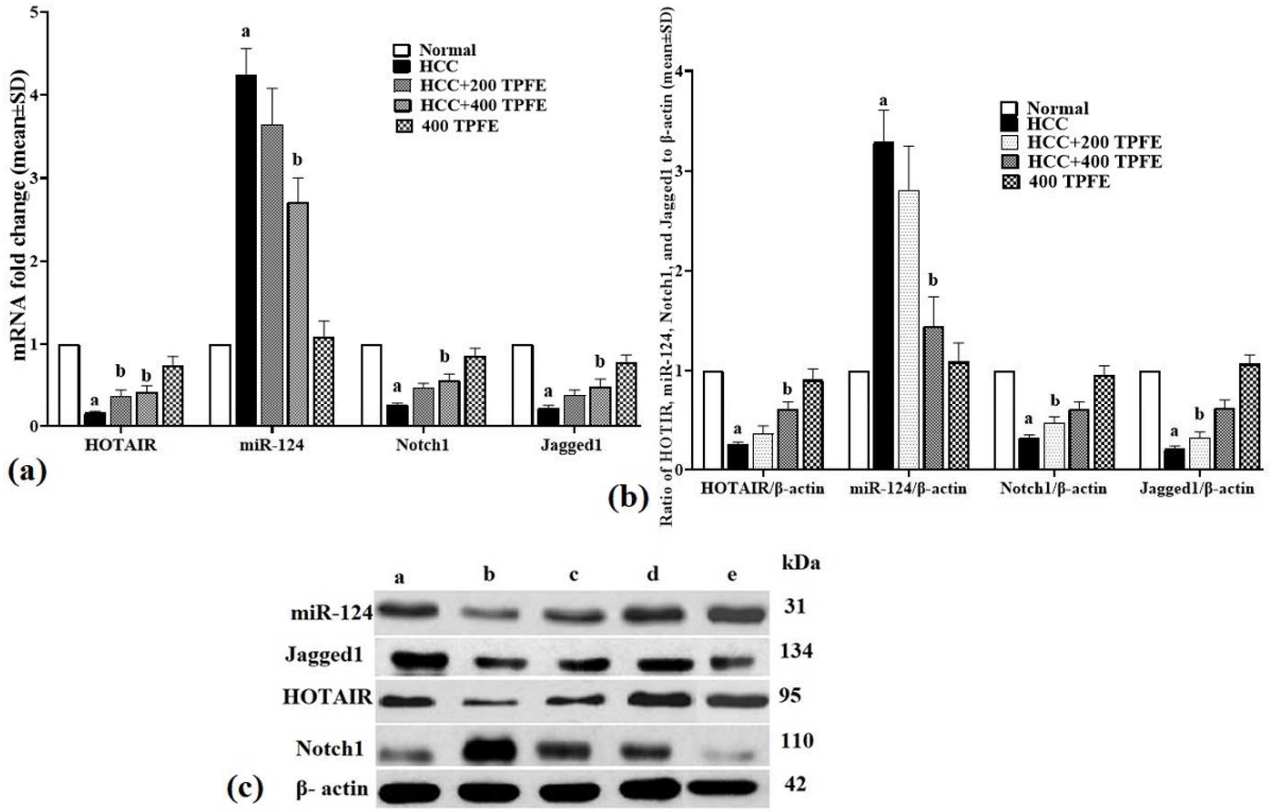

Fig. 3: (a) HOTAIR, miR-124, Notch1 and Jagged1 genes expression and (B, C) HOTAIR, miR-124, Notch1 and Jagged1 proteins expression in liver (means ± SD; n=10/group) in experimental groups. [a]($p<0.05$) HCC vs. normal groups; [b] ($p<0.05$) HCC+200 and 400 TPFE treated vs. HCC groups.

revealed that DEN treatment led to a significant decrease in the expression of HOTAIR, Notch1 and Jagged1, alongside an increase in miR-124 expression in hepatocytes compared to the control group ($p<0.05$). In the group treated with HCC+200 TPFE, there was an increase in the expression of HOTAIR, Notch1 and Jagged1, and a decrease in miR-124 expression compared to the HCC group, although these alterations did not reach statistical significance ($p>0.05$). The most remarkable changes were observed in the HCC+400 TPFE group, where HOTAIR, Notch1, and Jagged1 expression significantly rose, while miR-124 expression significantly dropped compared to the HCC group ($p<0.05$) (fig. 3a).

Expression of liver HOTAIR, miR-124, Notch1 and Jagged1 proteins

In order to thoroughly assess the influence of DEN on liver pathways related to proliferation, differentiation, and apoptosis, we examined the protein expression levels of HOTAIR, miR-124, Notch1 and Jagged1. Our analysis results indicated a significant decrease ($p<0.05$) in the protein expression of HOTAIR, Notch1 and Jagged1, coupled with a significant increase ($p<0.05$) in the protein expression of miR-124 compared to the control group. On the contrary, in the HCC+200 TPFE group, we observed an increase in the protein expression of HOTAIR, Notch1, and Jagged1, along with a decrease in the protein expression of miR-124 compared to the HCC group. Nevertheless, these changes did not demonstrate statistical significance ($p>0.05$). The most remarkable variations were noted in the HCC+400 TPFE group, where a significant increase ($p<0.05$) in the protein expression of HOTAIR, Notch1 and Jagged1 was observed, while a significant decrease ($p<0.05$) was noted in the protein expression of miR-124 compared to the DEN group (fig. 3b and fig. 3c).

Immunohistochemical and histopathological assessment

Liver p53 positive hepatocytes

An analysis of the findings on the percentage of cells positive for p53 indicated that DEN led to a notable rise ($p<0.05$) in the presence of these cells compared to the control group. Moreover, the cohorts exposed solely to 200 and 400 mg/kg of TPFE extract exhibited enhancements in apoptotic markers (decrease in p53-positive cells) in comparison to the HCC group. Notably, the decline in the percentage of p53-positive cells within the HCC+400 TPFE group demonstrated statistical significance when contrasted with the HCC group (fig. 4).

Liver histopathological evaluations

In the examination of liver tissue through histopathological analysis across the experimental groups, it was noted that DEN triggered hepatic degeneration

(HD) marked by lymphocytic infiltration (LI) and degenerated hepatocytes (D) surrounding the necrotic area. Within this particular group, there was an absence of the typical hepatic triad (HT) and hepatic lobule (HL). Conversely, in the HCC+200 and 400 TPFE groups, there was a restoration of hepatic lobule integrity to normalcy, coupled with a notable decrease in lymphocytic infiltration. Moreover, the presence of hepatic nodules was no longer evident in the liver, and the alignment of hepatocytes (H) adjacent to the liver sinusoids (S) was visibly restored. These alterations were observed to be dose-dependent, with the most prominent enhancement in tissue structure seen in the HCC+400 TPFE group (fig. 5).

DISCUSSION

The findings of this research highlight the efficacy of TPFE in preserving the optimal functionality of hepatocytes through its antioxidant, anti-inflammatory, and anti-apoptotic properties. Furthermore, TPFE holds potential in modulating the HOTAIR/miR-124/Notch1 pathway linked to DEN-induced HCC, thus offering protection against tumorigenic pathways in hepatocytes.

DEN significantly influences various signaling pathways related to apoptosis, autophagy and liver cell proliferation and differentiation. Studies indicate that DEN disrupts the PKB/AKT pathway, essential for hepatocyte function, while concurrently activating tumorigenic pathways such as Wnt/β-catenin and TGFβ-1/Smads, thus promoting hepatocellular tumorigenesis (Arboatti *et al*., 2019). The compound also triggers cyclin D1/MEK1,2 and the PI3K/Akt/mTOR pathways, further facilitating cancer development (He *et al*., 2023). Research highlights DEN's dual role in inhibiting the proliferation of both healthy and damaged hepatocytes through activation of the Bax/Bcl-2/p53 mitochondrial apoptosis pathway (Tang *et al*., 2020). Additionally, DEN initiates the ROS- and RNS-induced p53-dependent apoptotic pathway linked to cytochrome P450, resulting in caspase activation and subsequent cell death (Qsee *et al*., 2022). In the present study, DEN induced a decrease in antioxidant capacity and the activity of endogenous antioxidant enzymes, leading to increased lipid peroxidation compared to the normal group.

The free radicals generated by DEN triggered mitochondrial apoptosis and elevated the number of p53-positive cells in liver hepatocytes. The TPFE extract, especially at 400 mg/kg (in the HCC+400 TPFE treatment group), restrained inflammatory processes (characterized by reduced levels of IL-6, IL-1β, and TNF-α, alongside an elevation in IL-10) and alleviated oxidative stress (indicated by increased activity of GPx, SOD, and CAT and decreased NO levels) induced by DEN. Research suggests that TPFE acts as an antioxidant and inducer of apoptosis in cancer cells. It upregulates the expression of the Glutathione-S-transferase (GST) gene by mitigating DNA hyper-methylation, consequently inhibiting the proliferation of the prostate cancer cell line (PC-3) (Khazaei *et al*., 2017). A comparative evaluation of TPFE on human HL60 and HCT116 tumor cell lines underscores its anti-tumor properties, credited to its anthocyanin content, particularly delphinidin, which triggers tumor cell inhibition and programmed cell death (Wang *et al*., 2022a). In a research study by Muceniece *et al*. in 2019 focusing on the protective effects of TPFE against diazinon-induced liver damage, the plant extract exhibited a decline in hepatic enzyme levels (ALT, AST and ALP), safeguarding liver structure and function from oxidative harm by stimulating the activity of endogenous antioxidant enzymes (GPx, SOD, and CAT) (Muceniece *et al*., 2019). Akbaribazm *et al*. (2020b) explored the protective effects of TPFE against 4T1-induced breast cancer in mice, illustrating its capacity to reduce tissue levels of MDA, thiol, and NO while enhancing the activity of GPx and SOD (Akbaribazm *et al*., 2020b). Akbaribazm *et al*. (2020c) demonstrated that doses of 200 and 400mg/kg TPFE suppress inflammatory cytokines by inhibiting inflammatory pathways. Additionally, TPFE exhibits antioxidant properties by neutralizing free radicals and enhancing the activity of antioxidant enzymes, which helps protect the structure and function of hepatocytes. Furthermore, it was found to suppress the growth and metastasis of 4T1 breast cancer in tumor-bearing BALB/c mice (Akbaribazm *et al*., 2020c).

Moreover, DEN has been shown to induce hepatocyte necrosis and apoptosis through various pathways, including STAT3, P38, JNK, and JAK, along with factors such as cyclooxygenase-2 (COX-2) and IGF-2 (Gao *et al*., 2024). In this study, DEN induced the production of pro-inflammatory cytokines (TNF-α, IL-1β and IL-6) and inhibited the anti-inflammatory cytokine IL-10 compared to the normal group, triggering inflammatory processes in leukocytes and damaged cells. This exposure activates hepatic immune cells, such as macrophages and T helper (Th) cells, which play crucial roles in liver damage and tumor development. Activated macrophages secrete pro-inflammatory cytokines, contributing to a pro-inflammatory microenvironment and playing a dual role in cell clearance and tumor promotion. Th cells, particularly the Th1 and Th17 subtypes, also release cytokines that further influence the immune response. Key cytokines such as IL-6 and TNF-α are significantly upregulated following DEN exposure, promoting inflammation and potentially enhancing tumor progression (Gao *et al*., 2024; Ali *et al*., 2022). Furthermore, DEN promotes the release of proinflammatory cytokines (e.g., TNF-α and IL-6) while inhibiting anti-inflammatory cytokines, enhancing inflammatory pathways involving Kupffer cells and liver lymphocytes (Shaker *et al*., 2022).

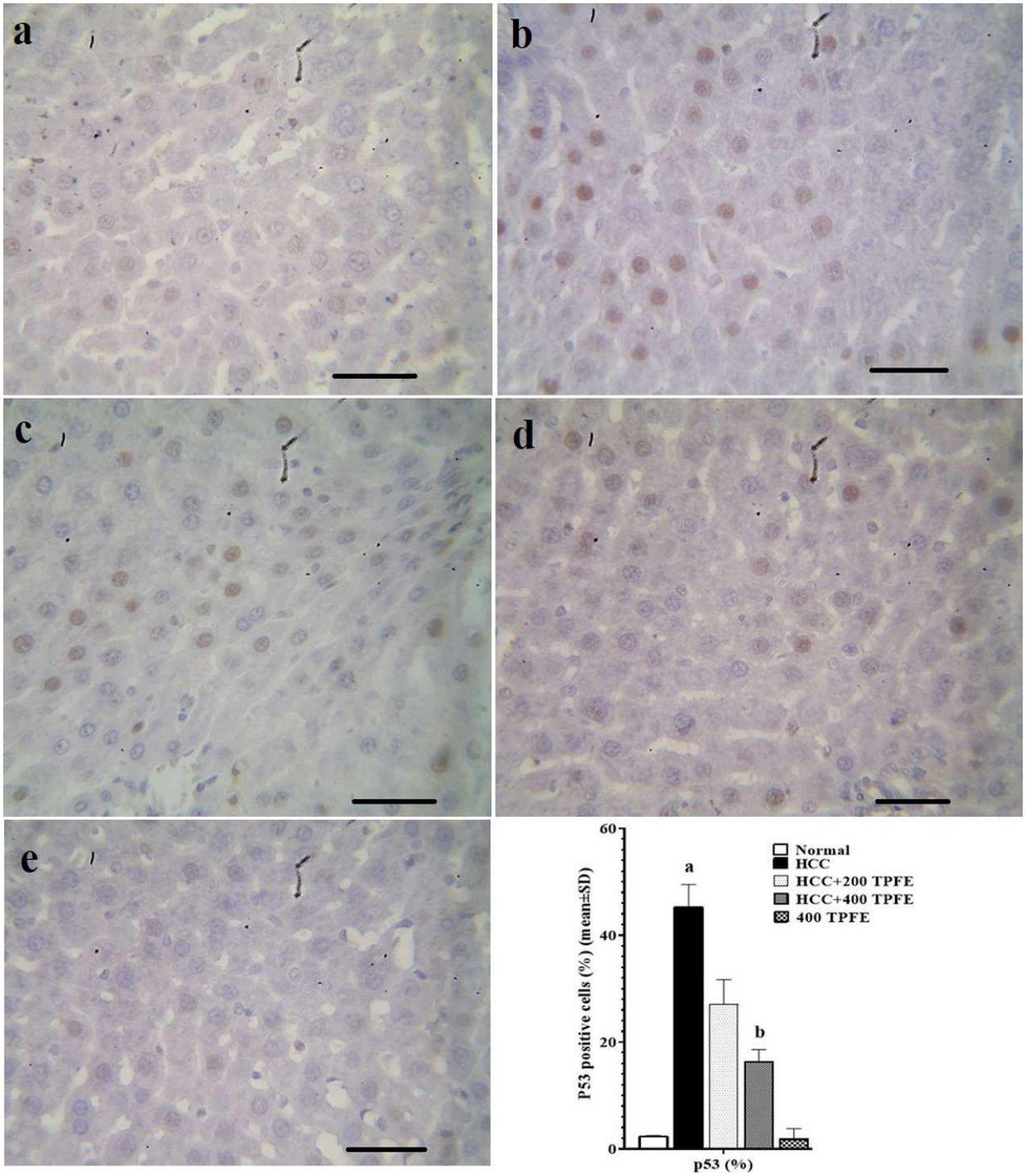

Fig. 4: p53 positive cells (%) in liver tissue by immunohistochemistry (n=10 rat/group, data are **"**means ± SD) (means ± SD; n=10/group) in normal (a), HCC (b), HCC+200 TPFE (c), HCC+400 TPFE (d), and 400 TPFE (× 100 with Scale bar = 200 µm)**.** [a] ($p<0.05$) HCC **vs.** normal groups; [b] ($p<0.05$) HCC+200 and 400 TPFE treated vs. HCC groups.

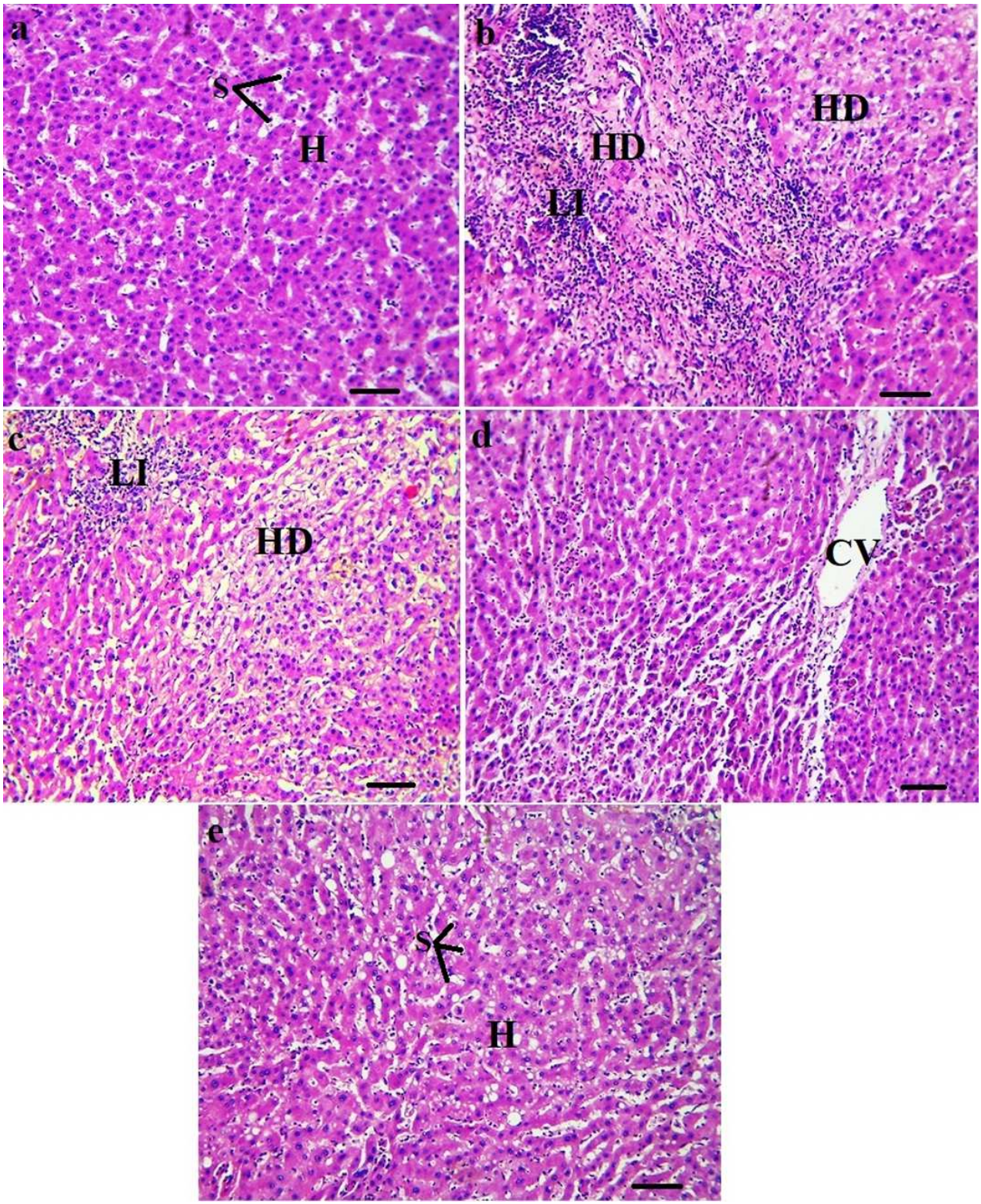

Fig. 5: Histopathological changes in liver tissue in normal (a), HCC (b), HCC+200 TPFE (c), HCC+400 TPFE (d), and 400 TPFE (e) (H & E, × 100 with Scale bar = 200 µm)**.** lymphatic infiltration (LI), central venule (CV), hepatic degeneration (HD), hepatic sinusoid's (S), normal hepatic (HL) and normal hepatocytes (H).

The HOTAIR/miR-124/Notch1 axis plays a critical role in regulating tumor cell dynamics, with DEN strengthening the NF-κB/COX-2 pathway, impacting hepatocyte function and promoting tumor progression (Ali *et al*., 2022). The results of the present study demonstrated that DEN disrupted the physiological function and structure of hepatocytes by inducing free radicals and inflammatory cytokines, ultimately leading to the suppression of the HOTAIR/miR-124/Notch1 metabolic axis in these cells. DEN increased the expression of miR-124, a tumor marker in hepatocytes, while simultaneously suppressing HOTAIR, Jagged1 and its receptor, Notch. These alterations in the metabolic axis rendered hepatocytes tumorigenic, resulting in changes to serum liver biochemical parameters, including ALT, AST, ALP, BIL, and CRP. The intricate components of liver function and disease involve the interplay of the HOTAIR/miR-124/Notch1 axis in liver cells, the insulin signaling pathway, and liver cancer development. HOTAIR, a long non-coding RNA (lncRNA), miR-124, a microRNA and Notch1, a transmembrane receptor, intricately regulate cellular functions in liver cells, such as growth and specialization, with their irregularities linked to the advancement of liver cancer (Price *et al*., 2021). Studies have shown that polyphenolic compounds present in TPFE, including formononetin, biochanin A, genistein and daidzein, can inhibit the metabolic, antioxidant, and apoptotic pathways associated with Nrf2/HO-1, RAGE/NLRP3, Bax/Bcl-2/Caspase-3 and the Beclin-1 pathway along the HOTAIR/miR-124/Notch1 axis (Shirvanian *et al*., 2024; Zafar *et al*., 2023). Biochanin A, found in TPFE, suppresses the growth and metastasis of cancer cells in HCC through the HOTAIR/miR-124/Notch1 pathway (Xiao *et al*., 2020). This compound, along with formononetin, inhibits the expression of matrix metalloproteinases (MMPs) such as MMP-2 and MMP-9 in cancer cells, thereby preventing metastasis (Wang *et al*., 2022b). Additionally, TPFE inhibits the metabolic and inflammatory pathways in cancer cells during HCC by targeting the IL-6/JAK/STAT3 pathway and regulating the expression of sirtuin-1/3 genes (Akbaribazm *et al*., 2022b). In the present study, TPFE effectively influenced miR-124 by augmenting the HOTAIR/Notch1/Jagged1 axis, thereby hindering the proliferation and specialization of cancerous cells. Furthermore, by strengthening the HOTAIR/Notch1/Jagged1 pathway that inhibits tumor growth, TPFE triggered programmed cell death in liver cells.

CONCLUSION

Our research highlights the potential of TPFE as a protective agent against DEN-induced HCC. Through a comprehensive examination of biochemical, molecular and antioxidant pathways, as well as its effects on the HOTAIR/miR-124/Notch1 axis, we have identified notable therapeutic advantages of TPFE. It appears that crude extracts or effective compounds derived from TPFE may be beneficial as prodrugs or supplements for patients with liver disorders, particularly HCC. However, further studies are needed to explore additional anticancer molecular mechanisms of TPFE, using various cancer models in both *in vivo* and *in vitro* settings. This research will help to establish a clearer understanding of the role of TPFE in cancer treatment.

ACKNOWLEDGMENTS

We extend our gratitude to the People's Hospital of HeChuan, Chongqing, The Third Affiliated Hospital of Zunyi Medical University, Zunyi and The First People's Hospital of Longquanyi District, Chengdu, for their support in conducting this study.

Conflict of interest

There is no conflict of interest.

Author's contribution

Chao-Du and Rubing-Deng contributed equally to this work.

REFERENCES

Akbaribazm M, Khazaei MR and Khazaei M (2020a). Phytochemicals and antioxidant activity of alcoholic/hydroalcoholic extract of *Trifolium pratense*. *Chin. Herb. Med.,* **12**(3): 326-35.

Akbaribazm M, Khazaei MR, Khazaei F and Khazaei M (2020b). Doxorubicin and *Trifolium pratense* L. (Red clover) extract synergistically inhibits brain and lung metastases in 4T1 tumor-bearing BALB/c mice. *Food Sci. Nutr.,* **8**(10): 5557-70.

Akbaribazm M, Khazaei MR and Khazaei M (2020c). *Trifolium pratense* L.(red clover) extract and doxorubicin synergistically inhibits proliferation of 4T1 breast cancer in tumor-bearing BALB/c mice through modulation of apoptosis and increase antioxidant and anti-inflammatory related pathways. *Food Sci. Nutr.,* **8**(8): 4276-90.

Al-Attar AM (2020). Therapeutic influences of almond oil on male rats exposed to a sublethal concentration of lead. *Saudi J. Biol. Sci.,* **27**(2): 581-7.

Ali G, Omar H, Hersi F, Abo-Youssef A, Ahmed O and Mohamed W (2022). The protective role of etoricoxib against diethylnitrosamine/2-acetylaminofluorene-induced hepatocarcinogenesis in wistar rats: The impact of NF-κB/COX-2/PGE2 signaling. *Curr. Mol. Pharmacol.,* **15**(1): 252-62.

Antonescu AI, Miere F, Fritea L, Ganea M, Zdrinca M, Dobjanschi L, Antonescu A, Vicas SI, Bodog F, Sindhu RK and Cavalu S (2021). Perspectives on the combined effects of *Ocimum basilicum* and *Trifolium pratense* extracts in terms of phytochemical profile and pharmacological effects. *Plants.,* **10**(7): 1390.

Arboatti AS, Lambertucci F, Sedlmeier MG, Pisani G, Monti J, Álvarez MD, Frances DE, Ronco MT and Carnovale CE (2019). Diethylnitrosamine enhances hepatic tumorigenic pathways in mice fed with high fat diet (Hfd). *Chem. Biol. Interact.,* **303**: 70-8.

Balaraman G, Sundaram J, Mari A, Krishnan P, Salam S, Subramaniam N, Sirajduddin I and Thiruvengadam D (2021). Farnesol alleviates diethyl nitrosamine induced inflammation and protects experimental rat hepatocellular carcinoma. *Environ. Toxicol.,* **36**(12): 2467-2474.

Chen K, Hou Y, Liao R, Li Y, Yang H and Gong J (2021). LncRNA SNHG6 promotes G1/S-phase transition in hepatocellular carcinoma by impairing miR-204-5p-mediated inhibition of E2F1. *Oncogene.,* **40**(18): 3217-30.

Fathi F, Sanei B, Ganjalikhani Hakemi M, Saidi RF and Rezaei A (2021). Liver resection promotes (regulates) proinflammatory cytokines in patients with hepatocellular carcinoma. *Can. J. Gastroenterol. Hepatol.,* **2021**(1): 5593655.

Gao M, Wang Y, Liu W, Song Z, Wang X and Zhang X (2024). Prunetin triggers ROS-mediated apoptosis through the suppression of MAPKs/STAT-3/NF-κB-p65 signaling pathway in human osteosarcoma Cells. *Pharmacogn. Mag.,* 09731296231188784.

Giovannini C, Fornari F, Piscaglia F and Gramantieri L (2021). Notch signaling regulation in HCC: From hepatitis virus to non-coding RNAs. *Cells.,* **10**(3): 521.

He J, Han J, Lin K, Wang J, Li G, Li X and Gao Y (2023). PTEN/AKT and Wnt/β-catenin signaling pathways regulate the proliferation of Lgr5+ cells in liver cancer. *Biochem. Biophys. Res. Commun.,* **683**: 149117.

Jing S, Kryger P and Boelt B (2021). Review of seed yield components and pollination conditions in red clover (*Trifolium pratense L.*) seed production. *Euphytica.,* **217**(4): 69.

Khazaei MR, Gravandi E, Ghanbari E, Niromand E and Khazaei M (2022). *Trifolium pratense* extract increases testosterone and improves sperm characteristics and antioxidant status in diabetic rats. *Biotech. Histochem.,* **97**(8): 576-583.

Khordad E, Akbaribazm M and Hosseini SM (2024). *Heracleum persicum L.* extract protects gentamicin-induced testicular toxicity. *Avicenna J. Phytomed.,* **14**(5): 585-599.

Konyn P, Ahmed A and Kim D (2021). Current epidemiology in hepatocellular carcinoma. *Expert Rev. Gastroenterol. Hepatol.,* **15**(11): 1295-307.

Price RL, Bhan A and Mandal SS (2021). HOTAIR beyond repression: In protein degradation, inflammation, DNA damage response and cell signaling. *DNA repair,* **105**: 103141.

Qsee HS, Tambe PK, De S and Bharati S (2022). MitoQ demonstrates connexin-and p53-mediated cancer chemoprevention in N-nitrosodiethylamine-induced hepatocarcinogenesis rodent model. *Toxicol. Appl. Pharmacol.,* **453**: 116211.

Muceniece R, Klavins L, Kviesis J, Jekabsons K, Rembergs R, Saleniece K, Dzirkale Z, Saulite L, Riekstina U and Klavins M (2019). Antioxidative, hypoglycaemic and hepatoprotective properties of five Vaccinium spp. berry pomace extracts. *J. Berry Res.,* **9**(2): 267-82.

Quah Y, Park NH, Lee EB, Lee KJ, Yi-Le JC, Ali MS and Park SC (2022). *Trifolium pratense* ethanolic extract alters the gut microbiota composition and regulates serum lipid profile in the ovariectomized rats. *BMC complement. Med. Ther.,* **22**(1): 5.

Shaker ME, Hamed MF and Shaaban AA (2022). Digoxin mitigates diethyl nitrosamine-induced acute liver injury in mice via limiting production of inflammatory mediators. *Saudi Pharm. J.,* **30**(3): 291-299.

Shirvanian K., Vali R, Farkhondeh T, Abderam A, Aschner M and Samarghandian S (2024). Genistein effects on various human disorders mediated via nrf2 signaling. *Curr. Mol. Med.,* **24**(1): 40-50.

Sumislawski P, Rotermund R, Klose S, Lautenbach A, Wefers AK, Soltwedel C, Mohammadi B, Jacobsen F, Mawrin C, Flitsch J and Saeger W (2022). ACTH-secreting pituitary carcinoma with TP53, NF1, ATRX and PTEN mutations Case report and review of the literature. *Endocrine.,* **76**(1): 228-236.

Tang Y, Cao J, Cai Z, An H, Li Y, Peng Y, Chen N, Luo A, Tao H and Li K (2022). Epigallocatechin gallate induces chemopreventive effects on rats with diethylnitrosamine-induced liver cancer via inhibition of cell division cycle 25A. *Mol. Med. Rep.,* **22**(5): 3873-85.

Wang B, Ma W and Di Y (2022a) Activation of the Nrf2/GPX4 signaling by pratensein from *Trifolium pretense* Mitigates ferroptosis in OGD/R-Insulted H9c2 Cardiomyocytes. *Nat. Prod. Commun.,* **17**(7): 1934578X221115313.

Wang JY, Jiang MW, Li MY, Zhang ZH, Xing Y, RiM and Jin X (2022b). Formononetin represses cervical tumorigenesis by interfering with the activation of PD-L1 through MYC and STAT3 down regulation. *J. Nutr. Biochem.,* **100**: 108899.

Wu C, Zhou S, Ma S and Suzuki K (2021). Effect of genistein supplementation on exercise-induced inflammation and oxidative stress in mice liver and skeletal muscle. *Medicina,* **57**(10): 1028.

Xiao Y, Gong Q, Wang W, Liu F, Kong Q, Pan F and Liu Y (2020). The combination of Biochanin A and SB590885 potentiates the inhibition of tumour progression in hepatocellular carcinoma. *Cancer Cell Int.,* **20**: 1-11.

Zafar S, Luo Y, Zhang L, Li CH, Khan A, Khan MI and Khan S (2023). Daidzein attenuated paclitaxel-induced neuropathic pain via the down-regulation of TRPV1/P2Y and up-regulation of Nrf2/HO-1 signaling. *Inflammopharmacology,* **31**(4): 1977-1992.

Zhang Y, Li X and Li X (2021a). Curcumae ameliorates diethylnitrosamine-induced hepatocellular carcinoma via alteration of oxidative stress, inflammation and gut microbiota. *J. Inflamm. Res.,* **14**: 5551-66.

Zhang Y, Aodeng G, Liu P, Su W and Zhao H (2021b). Effects of HOX transcript antisense intergenic RNA on the metastasis, epithelial-mesenchymal transition, and Notch signaling pathway in tongue cancer. *Transl. Cancer Res.,* **10**(1): 520.

Zughaibi TA, Suhail M, Tarique M and Tabrez S (2021). Targeting PI3K/Akt/mTOR pathway by different flavonoids: A cancer chemopreventive approach. *Int. J. Mol. Sci.,* **22**(22): 12455.